



EXPERIMENTAL AND NUMERICAL INVESTIGATION OF SLOT DIMPLE TUBE ON THE HEAT EXCHANGER PERFORMANCE

Humam K. Jalghaf¹ and Falah F. Hatem²

¹ Asst. Lecturer, Mechanical Eng. Dept., University of Technology, E-mail:
humam.karem@yahoo.com

² Lecturer, PhD, Mechanical Eng. Dept., University of Technology, E-mail:
falahhatem59@yahoo.com

ABSTRACT:

The present work investigated experimental and numerical the effect of internal radiate on the external tube on heat transfer coefficient and pressure drop in tube for range of Reynolds Number of (4000-16000). The study also discuss the different in results between the slot dimple tube and plain tube. Heat transfer and pressure drop for test tube were evaluated and presented as dimensionless value by Nusselt number and friction factor. Overall enhancement ratio of dimpled tube is discussed. Thermal and hydrodynamic results of CFD study are presented in form velocity vector and contour of local heat transfer coefficient. The results comparison of Nusselt number between plain tube and present slot dimples tube, shows that slot dimples tube enhance the heat transfer between 1.584 - 2 times the plain tube, and When compare between experimental and correlated Nusselt number for present slot dimple tube, the result show deviation in the test range of Reynolds number. The numerical results were in good agreement with the present experimental results. The deviation is within 6 - 22% higher for numerical at low and high Reynolds number, respectively. The overall enhancement ratio for present slot dimpled tube dependent on plain tube, the result depict that the slot dimple tube gave high enhancement in heat transfer relative to plain tube. The enhancement ratio is varied from (1.09 to 1.15) for range of Reynolds numbers between (4000 to 16000).

KEYWORDS: Experimental study, Numerical study, dimple tube, heat transfer enhancement, Nusselt number.

دراسة عملية ونظرية لاداء الانبوب ذي النذب الشقي المستخدم في مبادل حراري

م. د. فلاح فاخر حاتم

م. م. همام كريم جلعف

قسم الهندسة الميكانيكية، الجامعة التكنولوجية

قسم الهندسة الميكانيكية، الجامعة التكنولوجية

الخلاصة:

تم في هذا البحث دراسة تجريبية ونظرية لوجود نذب شقية طولية في انبوب مبادل حراري على ادائه لمدى من عدد رينولدز بين (4000 - 16000). تم في هذه الدراسة مقارنة النتائج بين أنبوب ذي النذب الشقي وأنبوب عادي كما تم تقييم انتقال الحرارة وانخفاض الضغط لأنبوب الاختبار وعرض كقيمة لابعدية بواسطة عدد نسلت ومعامل الاحتكاك. كذلك تم دراسة نسبة التحسين الكلية لانتقال الحرارة في الأنبوب. تم اظهار النتائج الحرارية والهيدروديناميكية بشكل متجهات سرعه و كونتور معامل انتقال الحرارة الموقعي. من مقارنة نتائج عدد نسلت بين الأنبوب العادي وانبوب ذي النذب الشقي الحالي تبين أن النذب الشقي يمكن أن يعزز نقل الحرارة بمقدار (2- 1.584) اكبر من الأنبوب العادي، وعند مقارنة رقم نسلت بين التجريبية والتصحيحية للأنبوب ذي الشق، اظهرت النتائج انحراف في مجموعة اختبار عدد رينولدز. وكانت النتائج النظرية في تطابق جيد مع النتائج التجريبية الحالية وبنسبة انحراف هو ضمن (6-22%) اعلى من النتائج النظرية لاقل واعلى عدد رينولدز على التوالي. نتيجة الاختبار نسبة التحسن الكلية للانبوب ذي النذب الشقي الحالي مقارنة مع أنبوب الاعتيادي، أن الأنبوب ذي النذب الشقي يعطي تعزيز عالي في نسبة التحسن الكلية بمقدار زيادة من (1.09-1.15%) لمجموعة من عدد رينولدز بين (4000-16000).

1. INTRODUCTION

Nowadays, a significant number of thermal engineering researchers are seeking for new enhancing heat transfer methods between surfaces and the surrounding fluid. Due to this fact, Bergles (1998), classified the mechanisms of enhancing heat transfer as active or passive methods, those which require external power to maintain the enhancement mechanism are named active methods. On the other hand, the passive enhancement methods are those which do not require external power to sustain the enhancements' characteristics. In addition, a hybrid technique which includes two or more form each of passive and active technique. Plain tubes are common elements used as a heat transfer surface in most heat exchange equipment. The overall heat transfer coefficient depends on both internal and external heat transfer process, for example, in fire tube boiler where flue gas passes through tube and water boiling takes place at the outer surface of tube. The heat transfer is restricted by the flue gas side due to lower thermal conductivity compared to boiling heat transfer which is almost greater than gas convective heat transfer by order of 30-50, therefore the enhancement be considered in tube side. In shell and tube heat exchanger, the convection heat transfer coefficient on the shell side (flow over the tubes) is 100-200% greater than the convective heat transfer coefficient inside the tube for the same Reynolds number, therefore, the enhancement of heat transfer at the internal tube surface is necessary to reduce the overall resistance of heat transfer.

Literature shows that an extensive work was developed to enhance the convective heat transfer coefficient inside tube. Watchorn et al. (2006) studied experimentally the influences of the twisted tape insertion on the heat transfer and flow friction characteristics in a concentric double pipe heat exchanger for the range of Reynolds number of 2000-12000. The experimental results revealed that the increase in heat transfer rate of the twisted-tape inserts is found to be strongly influenced by tape-induced swirl or vortex motion. Over the range investigated, the maximum Nusselt numbers for using the enhancement devices with $y = 5.0$ and 7.0 are 188% and 159%, respectively, higher than that for the plain tube. The swirling flow induced by twisted tape inserts led to high friction of 3.37 and 2.94 times of the plain tube, for $y = 5.0$ and 7.0 , respectively. Emman (2004) presented a numerical and experimental study on heat transfer enhancement by using semi-circular buckling (bulge) pipes. These buckling were organized in two ways in-line and stagger. The pipe is 0.0415m with buckling diameter of 0.022m and Reynolds number range 4000-30000. The study showed that the heat transfer rate increases with the increase in the buckling diameter. The study also indicates that the space between two buckling centres is inversely proportional to the heat transfer rate. The pressure drop in the

stagger is higher than that of in-line because this is more acute than the stagger due to higher velocity occur at the buckling surface. This higher velocity leads to higher-pressure drop, till the fluid reaches the top of the semi-circular buckling surface. Also her results show that the pumping power required for the stagger arrange is less than the inline due to previous reasons. [Khalil et al. \(2010\)](#) investigated experimentally the heat transfer, pressure drop characteristics, and efficiency enhancement for swirling flow through a sudden pipe expansion. Propeller swirl generator with different vane angles inserted at different distances (S) from the test pipe entrance to investigate its influence on the heat transfer inside the sudden pipe expansion. It was found that inserting a swirl generator inside a sudden pipe expansion causes an increment in both the relative mean Nusselt number and the enhanced efficiency of the tested pipe. [Amer et al. \(2016\)](#) investigated experimentally the heat transfer and pressure drop using dimpled tube. The experimental results showed that the heat transfer and pressure drop of staggered arrangement are increased when dimples pitch ratio X/d is decreased. The result also shows that the spherical dimple is the better than oval (with the same conditions), and the staggered arrangement performed better heat transfer than that of the inline arrangement. The current study is used slot dimpled tube and compared with plain tube. Evaluation the enhancement in heat transfer for slot dimpled through the study and the effect of increasing Reynolds number on Nusselt number with a constant surface temperature. The theoretical analysis of this work will be completed, using ANSYS FLUENT commercial CFD software to study the effect of Reynolds number on heat transfer enhancement, average Nusselt number and velocity profile.

2. TEST RIG AND EXPERIMENTAL APPARATUS:

The test rig composed of the following main parts and measuring apparatus, the schematic diagram and photo of the experimental apparatus used in this study are shown in [Fig. 1](#):

A: Flow System;

B: Steam Generation System;

C: Instrumentations.

A- Flow System

In the experimental, a turbulent flow regime was considered; therefore the system was designed for obtaining Reynolds number in the range of 4000 to 16000. The air flow system includes the following parts:

1. Blower.

2. Air flow tube
3. Test section.
4. Test tubes.

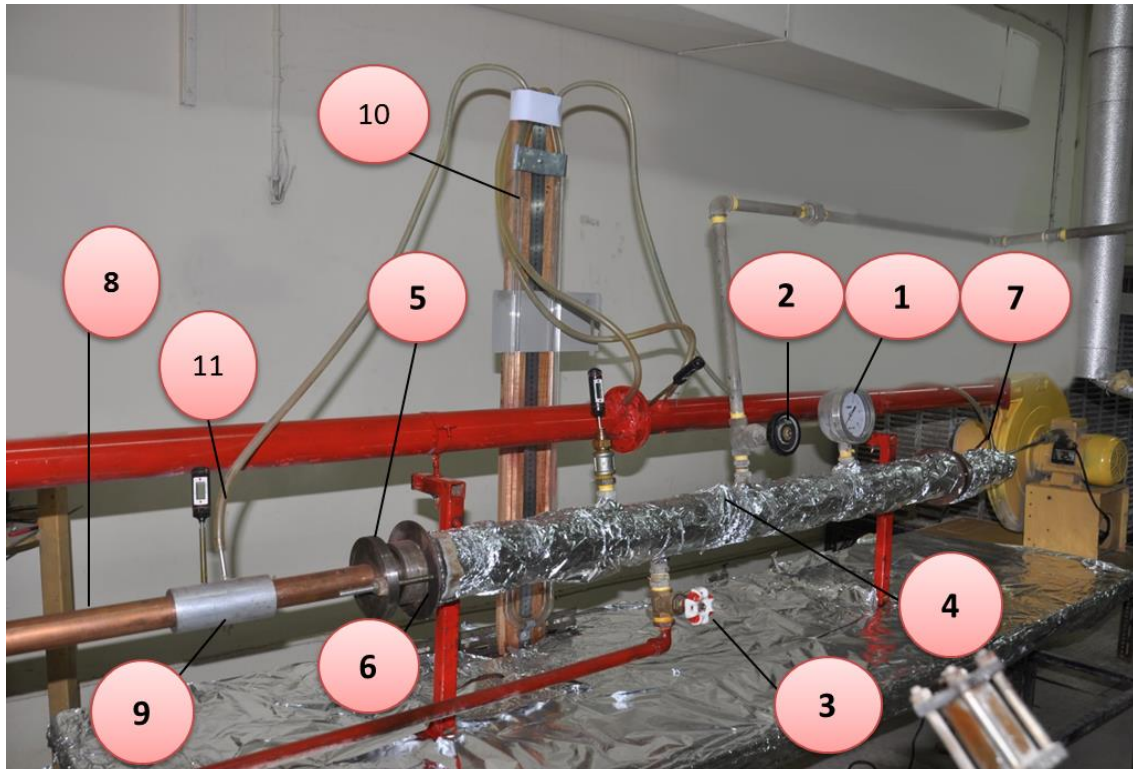


Fig. 1. The photos and Schematic diagram of the test rig

- 1- Borden gauge. 2- Steam delivers. 3- Steam condensate drain. 4- Steam shell with insulation.
 5- Flange of steam the shell. 6- Flange of the ring. 7-Outer air tube. 8- Inlet air tube. 9- Union joint.
 10- Water manometer. 11- Pressure tapping

The following notes classify technical description for each part:

1-Blower

Centrifugal fan with impeller diameter (410 mm) was used for supplying air to the test section. The fan is capable to provide volume flow rate of 40 m³/hr and the maximum discharge pressure of 4000Pa. The fan is driven by an electric motor of 500W running at 2800 r.p.m. The air flow rate is controlled by a slide vane located at the fan's inlet section.

2-Air Flow Tube

Air flow was measured using orifice flow meters manufactured according to British standard (Amer et al., 2016), This required a uniform and fully developed flow upstream of the orifice

section where L/D should be ≥ 16 , therefore a steel tube of (50 mm) inner diameter and (1000 mm) length is connected between the blower outlet flange and the orifice flange. Due to limited space, the test section is located in parallel to the air supply system, therefore a tube with U shape of 1 length on both side is connected between the orifice plate and the test section. This connection maintain the flow undisturbed downstream of the orifice plate and obtain a fully developed flow at the test section entrance. Pipe fitting reducer of 50 x 40 mm is connected with the U shape section to fit the diameter of the tube test section. This tube is connected with the test tube by special pipe coupling, where the pressure and temperature taps are fixed to connect with measurement apparatus.

3- Test Section: The test section contained of two parts:

I-Shell side

The test section is a shell and tube configuration, where steam flows in shell side, while air flows inside the tube. The shell side is made from carbon steel tube of 75 mm inner diameter, outer diameter 82 mm and 1200 mm length. The shell ends are welded with the special flange that machined to produce sealing housing, where sealing cap pushed through by screw bolts, the cross section of the flange and sealing cup. The flanges have a central bore hole with a diameter equal to the test tube diameter, where the test tube can be slide through aligning the tube to be in the shell center. Teflon rope of 10 mm is packed in the flange housing and warping round the test tube while sealing cup is forced by the four bolts to compress the teflon rope on the test tube and on the inner ring of the flange housing to produce tight sealing and to maintain the saturation steam pressure and temperature.

II-Test Tubes

Tube made from copper of 35 mm diameter and (1600 mm) long, as plain tube and then form a slot grove with (40mm) center to center distance, 5mm radius of slot and 5 mm grove depth, as shown in [Fig. 2](#), the tube was manufactured by CNC machine in the University of Technology Training Center.

B. Steam Generation System

In the present work, a fire tube boiler was used to produce a complete saturated steam. The boiler is equipped with fully automatic burner, safety controls, other tube fittings and measuring instruments. Steam is supplied at pressure up to 12bar and temperature 191.7°C. The saturated steam was supplied to the test section from the boiler via throttling valve and flow regulation

valve. The steam conditions at the inlet to the test section can be controlled for the desired pressure and temperature.

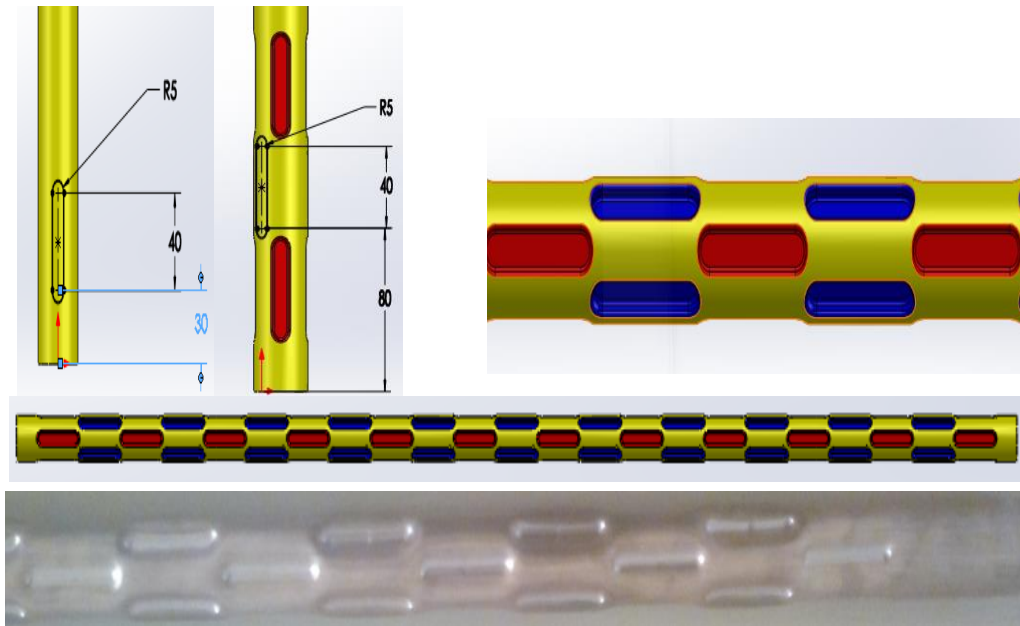


Fig. 2. The photos of the test tube.

C. Instrumentations

The essential measurements required are volume flow rate, temperature of air and steam, and pressure drop through test tube. The following sections describe the instrumentation that had been used in the experimental test:

1. Air flow rate instrument: Air flow rate was measured by orifice plate manufactured according to British Standard 1042 (British Standard, 199). The pressure tap is connected with water manometer by flexible polyethylene tube .
2. Temperature Instrument: Four digital thermometers type K were used to measure the temperature. The thermocouples were calibrated using standard calibration method. The accuracy of this thermometer was found to be of $\pm 0.1^{\circ}\text{C}$ for the range of temperature 0 to 300°C . These thermocouples were fixed at the following positions: One thermocouple placed upstream of the orifice plate. Two thermocouples were placed across the test tube to measure the inlet and the outlet air temperature. One thermocouple placed in the steam shell to measure the saturated steam temperature which represents the wall temperature of the test tube.
3. Pressure Instrument: Two types of pressure instruments were used:

- a) Borden gauge produced by (Amet) range of (0-10 bar) with increments of 0.2bar was used to measure the saturated steam pressure in steam shell.
- b) Two water manometers of range (1000mm water) were used to measure the pressure difference across the orifice plate and the pressure drop through test tubes.

3. CALCULATIONS

3.1. Volume discharge, mass flow rate, and mean velocity (Victor and Benjamin, 1984):

Volume discharge:

$$Q = C \cdot A_o \sqrt{\frac{2(p_2 - p_1)}{\rho}} \quad (1)$$

Where: C is the discharge coefficient obtained from chart at certain Reynolds number and area ratio.

Mass flow rate of air:

$$m = Q \cdot \rho \quad (2)$$

Mean velocity:

$$u_m = \frac{m}{A_c \cdot \rho} \quad (3)$$

Where:

$$A_c = \left(\frac{\pi}{4}\right) * (D_h)^2$$

3.2. Heat transfer calculation (Holman, 1976):

A –Heat transfer coefficient:

Energy balance gives the following equation:

$$Q \text{ (Wall)} = Q \text{ (air)}$$

$$\bar{h} \cdot A_s \cdot (LMTD) = m \cdot c_p \cdot (T_{ao} - T_{ai})$$

$$\bar{h} = \frac{m \cdot c_p \cdot (T_{\infty} - T_{ai})}{A_s \cdot (LMTD)} \quad (4)$$

Where:

$$A_s = \pi * D_h * L$$

Where: (LMTD) represents logarithmic mean temperature difference which is more accurate than average temperature when temperature increases higher than 50% (Shah, 1978), it is calculated as follow:

$$LMTD = \frac{(T_w - T_{ao}) - (T_w - T_{ai})}{\ln((T_w - T_{ao}) / (T_w - T_{ai}))} \tag{5}$$

3.3. Nusselt number (Nu):

$$Nu = \frac{h_a D}{k_a} \tag{6}$$

Then, the Nusselt number of smooth tube was calculated for comparison:

$$Nu = 0.023 Re^{4/5} Pr^n \quad \text{Dittus –Boelter equation (Frank and David, 1986)} \tag{7}$$

Where (n=0.4) for heating.

3.4. Friction factor (f) :

$$\frac{\Delta P}{\gamma} = f \frac{L}{D} \frac{\bar{u}^2}{2g} \quad \text{Darcy- Weisbach equation (Robert and Alan, 1998)} \tag{8}$$

Where : $\gamma = \rho * g$

Then, the friction factor of smooth tube was calculated for comparison:

$$f = \frac{0.316}{Re^{0.25}} \quad \text{Blasius equation. (Robert and Alan, 1998)} \tag{9}$$

3.5. Data Reduction

Heat transfer represented by dimensionless parameter Nusselt number is calculated by the using equation (6). To validate the present experimental test apparatus the test was performed on a plain tube, and the results are compared with well-known equations of Dittus-Boelter, Gueblink and Blasius equation for heat transfer inside a tube for a turbulent flow at constant wall temperature (Jafari et al., 2002).

$$Nu_u = 0.023 Re^{0.8} Pr^{0.3} \tag{10}$$

$$Nu_u = 0.012(Re^{0.87} - 280)Pr^{0.4} \tag{10a}$$

$$f = \frac{0.316}{Re^{0.25}} \tag{10b}$$

The friction factor can be defined on the basis of an equivalent shear force in the flow direction per unit of heat transfer (or friction area), whether this equivalent shear force is a true viscous shear or a primarily a pressure force. For the surface considered, the pressure drop across the tube is due to the viscous shear, turbulence and eddies induced by dimples. The friction factor (f) can be calculated by measuring the pressure upstream and downstream of the tested tube and according to the equation:

$$f = \frac{2 \Delta P D}{L \rho U^2} \quad (11)$$

And, Δp represents the pressure drop across the test section and is evaluated from the following equation:

$$\Delta P = \rho g h \quad (12)$$

The data obtained from the slot dimple tube were compared with plain tube for smooth pipe and the results presented later.

3.6. Overall enhancement ratio

Overall enhancement ratio is defined as the ratio of heat transfer enhancement ratio to the friction factor ratio based on the equal pumping power. This parameter is used to differentiate the passive technique and a comparison of different configurations for the technique itself. The overall enhancement ratio is defined as [Amer et al. \(2016\) \[5\]](#):

$$\eta = \left(\frac{Nue}{Nup} \right) / \left(\frac{fe}{fp} \right)^{0.3} \geq 1 \quad (13)$$

This relation based on the heat transfer and pressure drop of plain tube, and according to above relation, the overall enhancement ratio should be greater than unit. The greater value indicates better performance for that geometry, while value less than one indicate bad or worthless approach.

4. NUMERICAL APPROACH:

The numerical simulations or computational fluid dynamic CFD allow analysis of a complex phenomenon without resorting to an expensive prototype for flow visualization with sophisticated experimental measurements. In this section, geometry, mesh, setup (assumption, governing equations, turbulence model and boundary condition), solution and post processor results are discussed.

4.1. System Geometry:

The configurations of geometry are tube in dimensions (35mm diameter and 1600mm length), slot dimple dimensions (40 mm center to center distance, 5mm slot end radius and 5 mm depth). The system geometry is drawn by using (solid works) as shown in Fig. 2.

4.2. Mesh

Unstructured grids are in general successful for complex geometries, so for the above reason the unstructured tetrahedron grids was used in the current study. In the present work, a higher order element type, as shown in Fig. 3 is used for mesh generation to approximate precisely the boundaries of high curvature.

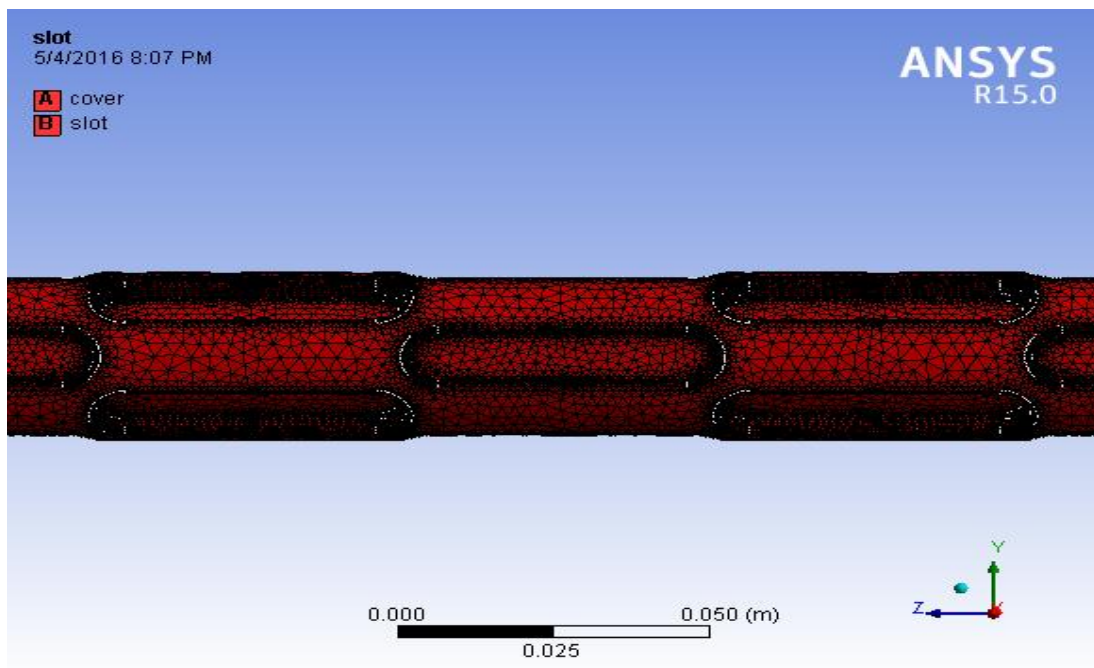


Fig. 3. Geometry mesh

- **Grid independence test:**

The final point in a good mesh is the total number of cells generated. It is vital to have enough number of cells for a good resolution but memory requirements increase as the number of cells increases. For the present cases, an average of (1.2) million cells is used.

4.3. Setup

4.3.1. Assumption:

In the present study, air is taken as the working fluid and the flow characteristics are assumed to be as (Steady flow, three dimensional, Newtonian fluid, Incompressible fluid, Turbulent flow).

4.3.2. Governing Equations:

The governing equations to be solved are the continuity, momentum, energy equations (Versteeg and Malalasekera, 1996) and (Roy, 1987). The mass of a fluid is conserved. The rate of change in the momentum is equal to the sum of forces on a fluid particle. The rate of change of energy is equal to the sum of the rate of the heat added to and the rate of work done on a fluid particle.

A. Continuity equation (Ashish and Shane, 2006)

$$\frac{\partial}{\partial x} \rho u + \frac{\partial}{\partial y} \rho v + \frac{\partial}{\partial z} \rho w = 0 \quad (14)$$

B. Conservation of momentum (Ashish and Shane, 2006)

$$\frac{\partial}{\partial x} \rho u^2 + \frac{\partial}{\partial y} \rho uv + \frac{\partial}{\partial z} \rho uw = -\frac{\partial p}{\partial x} + \frac{\partial}{\partial x} \mu_e \frac{\partial u}{\partial x} + \frac{\partial}{\partial y} \mu_e \frac{\partial u}{\partial y} + \frac{\partial}{\partial z} \mu_e \frac{\partial u}{\partial z} + S_x \quad (15)$$

$$\frac{\partial}{\partial x} \rho vu + \frac{\partial}{\partial y} \rho v^2 + \frac{\partial}{\partial z} \rho vw = -\frac{\partial p}{\partial y} + \frac{\partial}{\partial x} \mu_e \frac{\partial v}{\partial x} + \frac{\partial}{\partial y} \mu_e \frac{\partial v}{\partial y} + \frac{\partial}{\partial z} \mu_e \frac{\partial v}{\partial z} + S_y \quad (16)$$

$$\frac{\partial}{\partial x} \rho wu + \frac{\partial}{\partial y} \rho wv + \frac{\partial}{\partial z} \rho w^2 = -\frac{\partial p}{\partial z} + \frac{\partial}{\partial x} \mu_e \frac{\partial w}{\partial x} + \frac{\partial}{\partial y} \mu_e \frac{\partial w}{\partial y} + \frac{\partial}{\partial z} \mu_e \frac{\partial w}{\partial z} + S_z \quad (17)$$

C. Conservation of energy:[15]

$$\frac{\partial}{\partial x} \rho uT + \frac{\partial}{\partial y} \rho vT + \frac{\partial}{\partial z} \rho wT = \frac{\partial}{\partial x} (\rho \Gamma_e \frac{\partial T}{\partial x}) + \frac{\partial}{\partial y} (\rho \Gamma_e \frac{\partial T}{\partial y}) + \frac{\partial}{\partial z} (\rho \Gamma_e \frac{\partial T}{\partial z}) \quad (18)$$

Where, $\Gamma_e = \Gamma_1 + \Gamma_t$ and $\Gamma_1 = \frac{\mu_1}{Pr_1}$; $\Gamma_t = \frac{\mu_t}{Pr_t}$

4.3.3. Turbulence Model

The choice of turbulent model depends on consideration such as the physics encompassed in the flow, the established practice for a specific class of problem, the level of accuracy required, the available computational resources, and the amount of time available for the simulation. To make the most suitable choice of model for the application, it is necessary to understand the capabilities and limitations of the various turbulence models from previous researches. The standard ($k - \varepsilon$) model is economical with reasonable accuracy for a wide range of turbulent flows and it is widely used in heat transfer simulation.

4.4. Boundary Conditions

The boundaries are similar to the experiment and are prescribed at all boundary surfaces of the computation domain.

At solid walls, constant wall temperature boundary conditions are used with temperature of 135°C, and no-slip boundary condition is set for the geometry. Inlet velocity condition for the mainstream air inlet which set to have a uniform velocity profile. Five inlet velocity used to obtain Reynolds number value of (4000, 8000, 12000, and 16000), and at outlet set the boundary as pressure outlet.

4.5. Solution

The segregated solver, ANSYS is the solution algorithm used by FLUENT and is adopted in the present work. For high speed and compressible flows another solver, called coupled solver may be activated in FLUENT. Since no compressibility effects are introduced, this method (coupled solver) will not be investigated. Using segregated solver approach, the governing equations solved sequentially (i.e., segregated from one another). Since the governing equations are non-linear (and coupled), many iterations may be done before a converged solution is obtained. The SIMPLE algorithm is used in the present work.

4.5.4. Initial Condition

The flow field is unknown unless iteration is started; therefore, an initial guess is needed to start the solution. The initialization of the model is important for convergence. If the initial conditions are poor, then it takes longer to converge or it may even result in divergence. For the present work, all variables are initiated from the inlet boundary conditions.

5. RESULTS AND DISCUSSION

In this section, the experimental and numerical results of slot dimple tube presented. Heat transfer and pressure drop for test tube were evaluated and presented as dimensionless values by Nusselt number and friction factor for the range of Reynolds number from 4000 to 16000. Overall enhancement ratios of dimpled tube discussed. Thermal and hydrodynamic results of CFD study are presented in form velocity vector and contour, contour of local heat transfer coefficient, turbulent kinetic energy and turbulence intensity.

A. The local heat transfer coefficient on slot dimples and plain surface

It is clear that high heat transfer can be observed on the dimples surfaces and at the surface downstream of the dimpled body due to the flow impingent and reattachments at these regions

where high turbulence are existing, the heat transfer in dimpled tube can be classified into two surfaces which are the dimples and the plain surface, and can be note that the maximum heat transfer coefficient occur at inlet of tube as shown in Fig. 4.

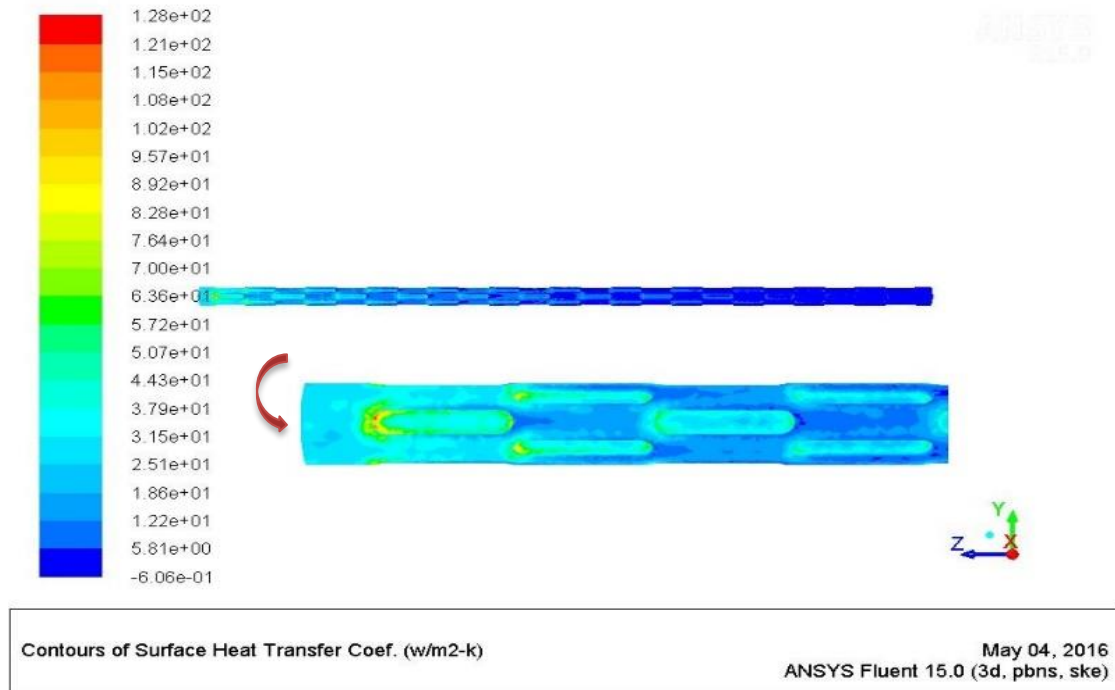


Fig. 4. Contour of heat transfer coefficient

The experimental Nusselt number for the present dimple tube are shown in Fig. 6, the Nusselt number increase with increase Reynold number which is natural behavior due to increase the turbulent flow which leads to destroy the flow pattern and the flow become more irregular and that allow to cool air in the core of flow to reach into the wall and this temperature difference allow to heat transfer between the flow and wall. While the friction factor decrease with the increase in the Reynold number because the dimple create pressure difference between the up and down of dimple, and arrange the slot dimple in staggered miner also leads to obstruction the flow as shown in Fig. 5. In general, for a laminar flow, the pressure differential across the protrusion is small in the absence of separation. Across the dimple dome, the pressure difference between the fore and aft side of the dimple is also small. Hence, at low Reynolds numbers, the shear or surface friction dominatess the total losses. For turbulent or high Reynolds number, flow separation and wake formation on the protrusion with separation and reattachment within the dimple. This is attributing to the high pressure associated with slot

dimpled tube compared with the plain tube. The mean friction factor for the dimple tube (5.87) times higher than that for the plain tube as shown in Fig. 8.

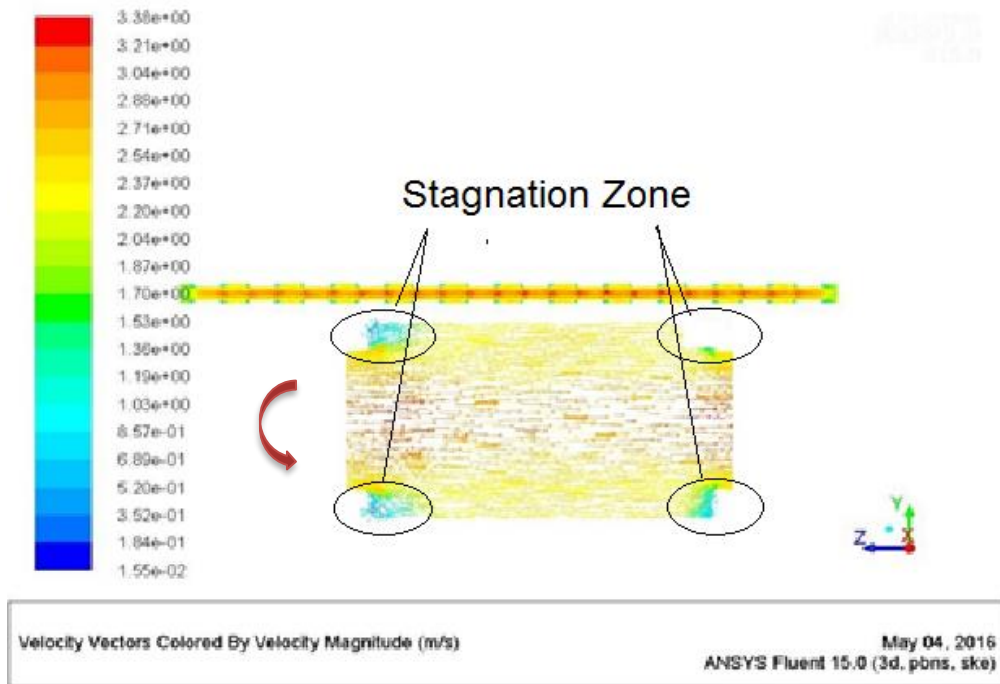


Fig .5. Velocity vector

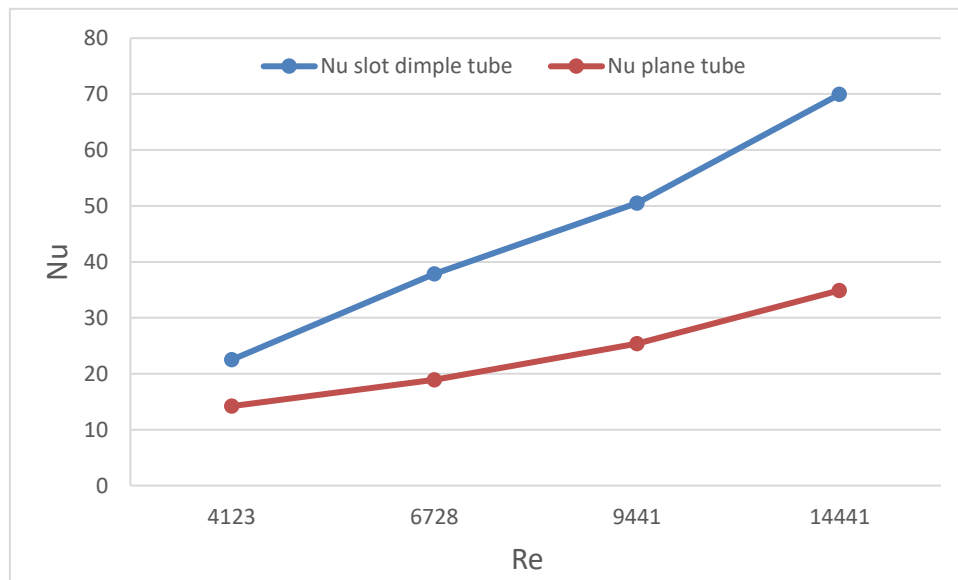
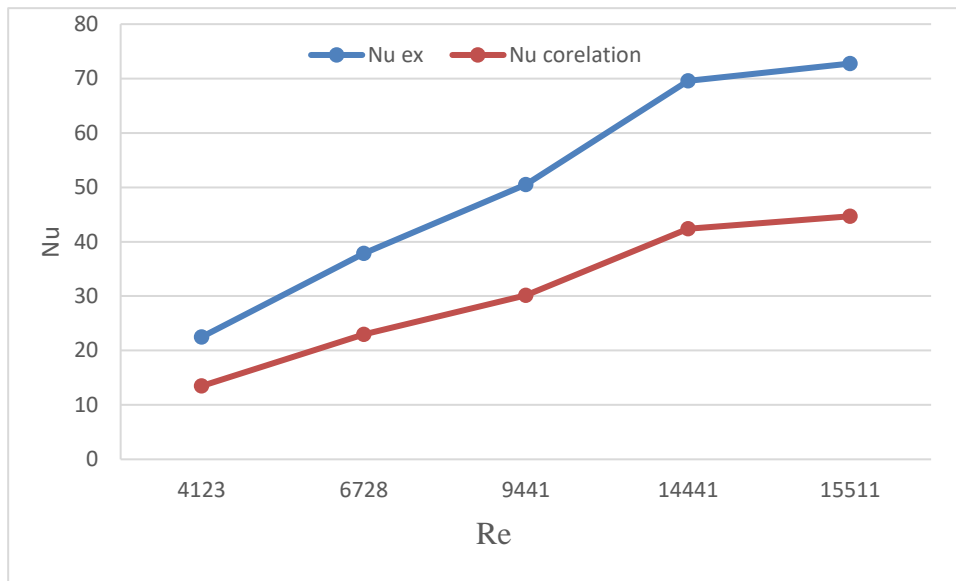


Fig. 6. Comparison between Nusselt number for the slot dimple tube and plain tube for the present experimental results

A- Comparison of enhancement technique

1. Heat transfer and pressure drop, Fig. 6 illustrates the Nusselt number of plain tube in comparison with the present slot dimples tube. the result show that slot dimples tube can enhance the heat transfer by 1.584- 2 times the plain tube, and when compare between experimental and correlation Nusselt number for present slot dimple tube as in Fig. 7, the result show deviation in the range of Reynolds number 4000-16000. The enhancement of heat transfer is accompanying with increase in pressure drop. Fig. 8 reveals the friction factor of the present slot dimples and plain tube technique. The result shows that the slot dimple tube has moderate pressure drop on dimple pitch. For both bulge and dimple tube, the existing of lump induced drag due to sudden change in flow directions, therefore pressure drop is proportion with lump depth. The numerical results were in good agreement with the present experimental results. Fig. 9 reveals the comparison between the numerical and experimental results of heat transfer for present slot dimple tube. The deviation is within 6- 22% higher for numerical at low and high Reynolds number, respectively. Fig. 5 Shows the variation of heat transfer along the tube, where high heat transfer can be noticed at the inlet section where a laminar boundary layer exists.
2. overall enhancement ratio: Fig. 10 shows the overall enhancement ratio for present slot dimpled tube dependent on plain tube. The result depict that the slot dimple tube give high enhancement in heat transfer relative to plane tube due to increase in heat transfer area. The enhancement ratio is varied from (1.09 to 1.15) for range of Reynolds numbers (4000-16000). This indicates that 9-15% of heat transfer area can be saved at the same pumping power compared with the plain tube heat exchanger.



**Fig. 7. Comparison between experimental and correlation Nusselt t number
For present slot dimple tube**

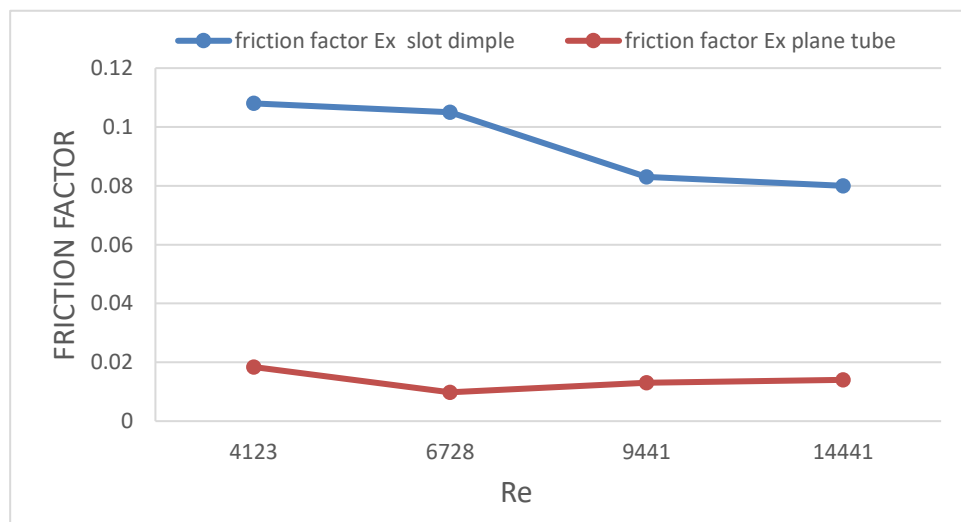


Fig. 8. Comparison experimental friction factor between present slot dimple tube and plain tube

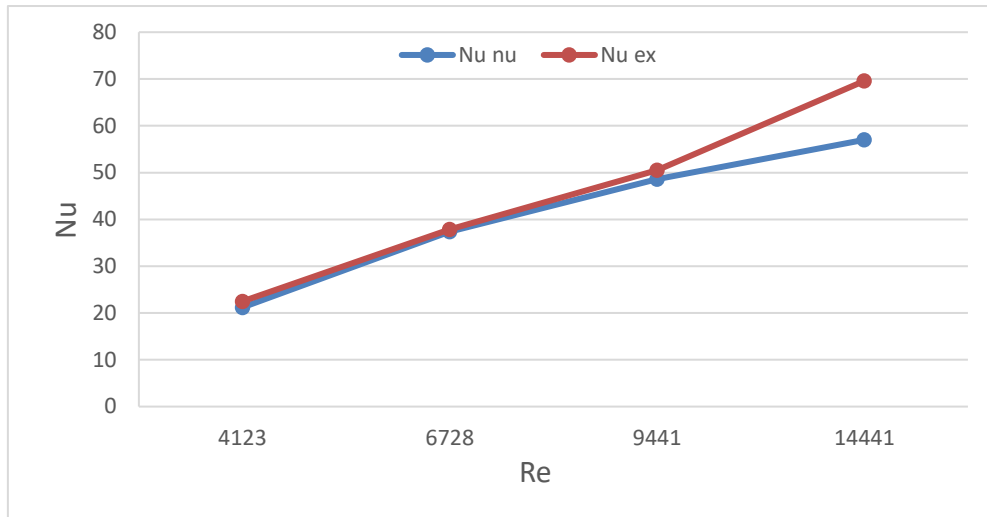


Fig. 9. Comparison between numerical and experimental Nusselt number for present slot dimple tube

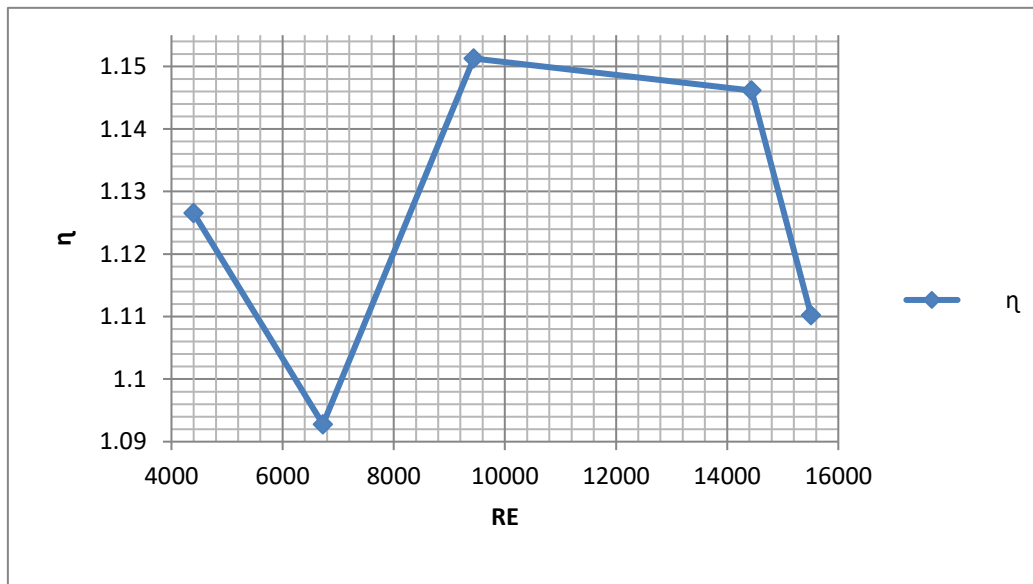


Fig. 10. The overall enhancement ratio for present slot dimpled dependent on plain tube

6. CONCLUSION

The present work reaches to the following conclusion:

1. Nusselt number increase with increase Reynold number due to increase the turbulent flow which leads to destroyed the flow pattern and the flow become more irregular
2. Friction factor decrease with increase in the Reynold number because the dimple create pressure difference between the upstream and downstream of dimple.
3. The numerical results were in good agreement with the present experimental results.

4. Use slot dimple tube give high enhancement in heat transfer relative to plane tube due to increase in heat transfer area.
5. Heat transfer area can be saved at the same pumping power compared with the plain tube heat exchanger.

7. NOMENCLATURES:

A	Orifice cross-sectional area	(m ²)
A _s	Tube surface area	(m ²)
C	Discharge coefficient	
C _p	Specific heat at constant pressure	(J/kg. k)
D	Tube diameter	(m)
L	Test section length	(m)
f	friction factor	
h	Average heat transfer coefficient	(W/ m ² .K)
m	Mass flow rate	(kg/s)
Nu	Average Nusselt number	
P	Pressure	(pa)
Pr	Prandtl number	
Q	Volumetric discharge	(m ³ /s)
q	Heat energy	(W)
T	Temperature	(c, K)
t	time	sec
u	Mean velocity	(m/s)
ρ	Fluid Density	kg/m ³

8. REFERENCES

Amer M. Al-Dabbagh, Falah F. Al-Jabery, & Hussain A. Jummaa, ,” Enhancement of Heat Exchanger Using Oval Dimpled Tube”, to be published during 2016.

Ashish Kulkarni and Shane Moeykens, "Introduction to FLUENT Note", Sixth edition, ANSYS Inc., November 2006

Bergles, A.E. Handbook of heat transfer, McGRAW-Hill, New York, NY, US, 3rd edition, 1998.

British standard 1042, 1992 "Measurement of flow through orifice plate".

Eman Hassan Mohammed. "Numerical and experimental investigation for heat transfer enhancement in boilers tube", M.Sc. thesis submitted to University of Technology Mechanical Engineering Department 2004.

Frank B. Incropera and David B. Doot, "Principles of Heat Transfer", Mc.Graw- Hill Company, 1986.

Holman J. P., "Heat Transfer", Fourth edition, McGraw-Hill Company, 1976.

Jafari Nasr M. R, Polley G. T., and Zoghi A. T., "Performance Evaluation of Heat Transfer Enhancement", CHISA, Prague, 2002.

Khalil, A. /E. Zohir and A.M. Farid," Heat transfer characteristics and friction of turbulent swirling air flow through abrupt expansion", American Journal of Scientific and Industrial Research, 1(2):p.p. 364-374, 2010.

Robert W. Fox and Alan T. McDonald, "Introduction to Fluid Mechanics", Fifth edition, John Wiley & Sons Inc, 1998.

Roy, D.N., 1987," Applied Fluid Mechanics", Affiliated East-West Private LTD, New Delhi.

Shah R. K., "Compact Heat Exchanger Surface Selection Methods" , Heat Transfer 1978, Proceedings of the Sixth International Heat Transfer Conference, Vol. 4, p.p. 193-199, Hemisphere Publishing Company, Washington, D. C.

Versteeg, H.K. and Malalasekera, W., 1996, "An Introduction to Computational Fluid Dynamics the Finite Volume Method", Longman Group, London.

Victor L. Streeter and E. Benjamin Wylie "Fluid Mechanics", Seventh edition, McGraw-Hill Company, 1984.

Watcharin Noothong, Smith Eiamsa-ard, and Pongjet Promvonge," Effect of Twisted-tape Inserts on Heat Transfer in a Tube", The 2nd Joint International Conference on "Sustainable Energy and Environment (SEE 2006)", 21-23 November 2006, Bangkok, Thailand.